SCIENCE CHINA
Technological Sciences

Special Topic: Smart and Functional Fiber Materials
•**Review**•

June 2019 Vol.62 No.6: 886–894
https://doi.org/10.1007/s11431-018-9405-5

Fabrication of nanofibrous sensors by electrospinning

HAN WeiHua[1], WANG YuZhi[1], SU JianMin[1], XIN Xin[2], GUO YinDa[2], LONG Yun-Ze[2*] & RAMAKRISHNA Seeram[3*]

[1] *Facility Horticulture Laboratory of Universities in Shandong, Weifang University of Science and Technology, Weifang 262700, China;*
[2] *College of Physics, Qingdao University, Qingdao 266071, China;*
[3] *Faculty of Engineering, National University of Singapore, Singapore 119077, Singapore*

Received October 17, 2018; accepted December 5, 2018; published online April 4, 2019

This article reviews the techniques and applications of electrospinning for the fabrication of nanofibrous sensors. Considering that nanosensors require a large specific surface area and a continuous structure for the conduction of current signals, electrospun nanofibers have the dominant advantage. The device preparation is mainly divided into surface treatment and high-temperature sintering, which are, respectively, used for preparing composite conductive fibers and inorganic semiconductor fibers. Typical applications include pressure sensing, gas sensing, photoelectric sensing, and temperature sensing. In addition, nano-self-powered systems have been mentioned to emphasize the good performance of smart nanosystems that do not require external power. In addition, we have summarized some existing methods and suggestions for increasing the specific surface area and presented constructive ideas for the future development of these devices.

smart nanofibers, electrospinning, conductive composite nanofibers, inorganic semiconductive nanofibers, sensors, self-powered device

Citation: Han W H, Wang Y Z, Su J M, et al. Fabrication of nanofibrous sensors by electrospinning. Sci China Tech Sci, 2019, 62: 886–894, https://doi.org/10.1007/s11431-018-9405-5

1 Introduction

Smart materials [1–4], which can also be called responsive materials, are a type of materials that possess properties that can be controlled by external stimuli. The stimuli can be pressure [5], temperature [6], pH [7], moisture [8], electric or magnetic fields [9], chemical compounds [10,11], or light [12,13]. When the response property is accessible to electronics, the material can work as a sensor [14–16]. When the response property is length or force, the material becomes an actuator/artificial muscle [17,18]. Whether it is future artificial intelligence or current automation control, data acquisition and conversion into computer-processable electrical signals are essential and require a large number of inexpensive but reliable sensors. In general, sensing occurs preferentially at the interface; therefore, sensors usually require a large specific surface area, while nanomaterials are materials with a large specific surface area, and their specific surface area can be increased rapidly by decreasing their dimensions. Another consideration is that a sensor usually needs to be assembled into a certain measuring instrument or analog-to-digital conversion circuit; therefore, it needs to form a stable continuous circuit to provide a path for the current. From this aspect, electrospinning is irreplaceable because of its ability to prepare continuous one-dimensional materials. It avoids complex micro-nano processing techniques and can be assembled using only conventional electrode connecting techniques.

Nanofibers have the advantages of light weight, continuous, large specific surface area, and easy loading of functionalized nanomaterials [19,20]. At present, there are various techniques for preparing nanofibers, such as the

*Corresponding authors (email: qdu_long@126.com; seeram@nus.edu.sg)

template method [21,22], self-assembly method [23], and etching method [24]. However, compared with the electrospinning technology, these methods produce structures with a complex interface [25], leading to extrinsic effects or high costs. Therefore, it is difficult to use these methods on inexpensive clothing. However, the electrospinning technology can solve this problem in essence. On one hand, this technique can produce a continuous nanofiber membrane at a low cost and with a relatively uniform fiber diameter. On the other hand, through the improved electrospinning technology, such as near-field electrospinning technology and high-speed drum collection technology [26,27], the configuration of the electrospun fiber can be well regulated, thereby realizing different designs.

In this review report, we will first introduce the application of the electrospinning technology for the preparation of nanosensors. Traditional pressure sensing, gas sensing, photoelectric sensing, and temperature sensing will be introduced next, followed by self-powered sensors using nanogenerators. Some constructive comments and outlooks will be provided at the end.

2 Preparation strategy

2.1 Electrospinning process

There are typically two synthesis strategies, as shown in Figure 1 [28,29]. A conventional electrospinning device includes a high-voltage power supply, a liquid supply system, and a collector. In the electrospinning process, as the spinning voltage increases, when the electric field force is greater than the surface tension of the solution, the charged solution is ejected from the spinneret to form a jet, and the jet reaches the receiving electrode under the action of the electrostatic field. In common cases, the parameters used in electrospinning are as follows: usually, the spinning voltage is controlled in the range of 10–30 kV, and the distance between the spinning needle and the receiving end is controlled within a distance of 10–50 cm. An increase in the voltage and an increase in the electrode spacing will decrease the diameter of the fiber to some extent. Because of the splitting of the jet and the fiber whip during the electrospinning process, ultrafine or even nanofibers are eventually formed. In general, the electrospinning process relies on a polymer material solution, so the direct spinning product is usually a soluble polymer material, which results in the electrospinning of the conductive fibers requiring subsequent processing.

2.2 Surface deposition

On the basis of the electrospun material, a certain conductive material can be deposited on the surface of the fiber to obtain a conductive fiber. These surface deposits include polymeric conductive materials, physical or chemical deposition, and surface coating of carbon nanotubes.

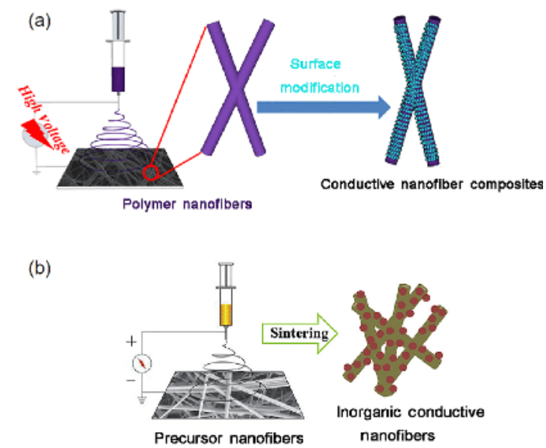

Figure 1 (Color online) Flow chart elaborating the preparation of conductive nanofibers by electrospinning. (a) Preparation of polymer composite conductive nanofibers [28]; (b) preparation of inorganic polymer conductive fibers [29].

2.3 Precursor heat treatment

In addition to the surface treatment, a certain precursor may be used for the heat treatment to obtain conductive fibers. The inorganic oxide fiber can be obtained by electrospinning a polymer such as polyvinylpyrrolidone (PVP) or polyvinyl alcohol (PVA) containing a metal complex, and then burning the polymer material in an air atmosphere. In contrast, polyacrylonitrile (PAN) is dissolved in N,N-dimethylformamide (DMF) for electrospinning, and after pre-oxidization in air and carbonization by insulating air, conductive carbon fibers can be obtained.

2.4 Percolation principle

In principle, a conductive material requires a conductive portion of the material to reach a percolation concentration to form a continuous conductive path. This results in the poor conductivity of fibers that are directly doped with conductive materials. However, if the nanofibers are treated only on the surface by a conductive material, a cylindrical structure is formed, the conductive ability is retained, and a large specific surface area is obtained; thus, they exhibit a good response to substances such as a gas. In contrast, when the fibers are obtained by the precursor treatment, the polymer template is completely removed, and a continuous conductive material is obtained. Note that the two strategies are not mutually exclusive. For example, the electrochemical deposition of metals on carbon nanofibers can be used to fabricate nanofibers with a conductors's interface.

3. Applications

3.1 Pressure sensors

Nanofibers prepared by electrospinning tend to be fluffy. As a result, the shape of the conductor changes under the action of pressure, so the resistance of the fiber changes significantly when the resistivity is constant. Thus, by keeping the voltage at both ends of the fiber constant, the fiber current can characterize the change in pressure [27,30]. For example, Hu et al. [31] designed a silver-loaded sodium alginate fiber. Sodium alginate (0.64 g), polyethylene oxide (PEO) (0.16 g), Triton X-100 (0.4 g), and dimethyl sulfoxide (2 g) were dissolved in water (36.8 g) for electrospinning, and the fibers were then immersed in a silver nitrate solution (25 wt%). Finally, reduction was carried out using dimethylamine borane to obtain a silver-loaded sodium alginate fiber. This fiber showed a good response to pressure, and reproducibility experiments showed that it has good resilience and hence can be used accurately and repeatedly for pressure sensing, as shown in Figure 2 [31]. Applying the sensor to the chest and throat revealed that the fibers indicated breathing and language well. By using a scanning circuit, we can convert these sensors into a pressure sensing unit to prepare an electronic skin, which is capable of characterizing the pressure distribution [31].

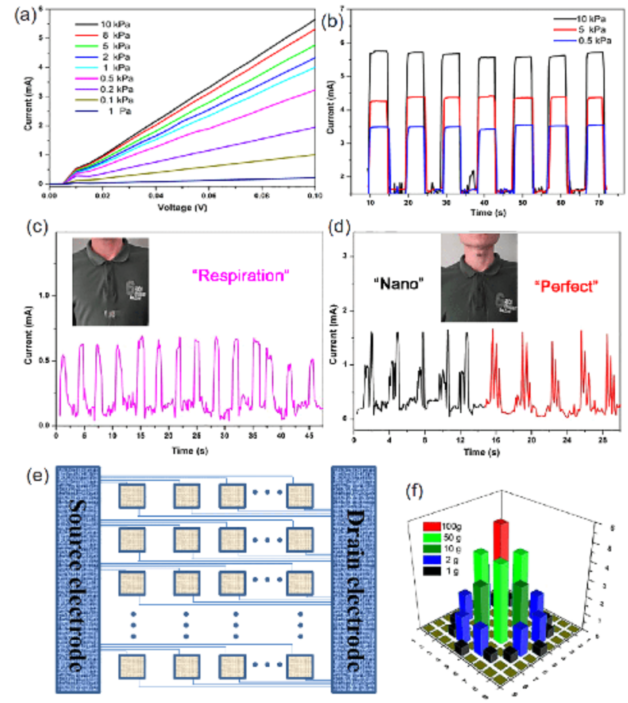

Figure 2 (Color online) Pressure sensing performance of silver-loaded sodium alginate nanofibers. (a) *I-V* plots under different pressure conditions; (b) response repeatability under different pressure conditions; (c) response to human respiration after the fiber is applied to the chest; (d) responses to the different words "Nano" and "Perfect" after the fibers are applied to the throat; (e) electrode array map for electronic skin; (f) mapping of the pressure signal [31].

Yu et al. [32] used a patterned collector to prepare a patterned stretchable stress sensor, as shown in Figure 3 [32]. First, polyvinylidene fluoride (PVDF) (dissolved in 1:1 N,N-dimethylformamide and acetone with a weight ratio of 22%) was deposited by electrospinning onto different patterned conductive mesh structures, such as hexagonal structures collectors, approximately rectangular collectors, metal meshes, and circular collectors, and then the obtained fibers. The PANI conductive polymer material was then polymerized onto the fibers to obtain a conductive fiber membrane. In addition to the common tensile sensing properties, the fabricated sensor exhibited considerably higher tensile properties than the conventional disordered fibers. The highest detectable strain was 110%, which was 2.6 times that of conventional disordered fibers. The reason for this effect was that collector patterning led to local electric field enhancement, which increased the overall strength of the fiber [32].

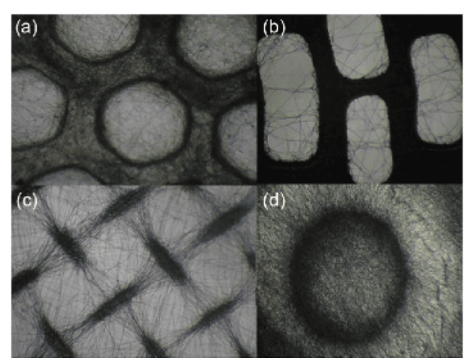

Figure 3 Different patterned membranes collected by different electrode configurations [32].

3.2 Gas sensors

In addition to stress sensing properties, the conductive material itself may experience a sensing response to the gas. Because of the large specific surface area of the nanofibers, this response can often eliminate complex internal diffusion processes and only complete the percolation limit on the surface to achieve rapid gas sensing. Zhang et al. [33] prepared zinc oxide nanowires by using chemical vapor deposition. These nanowires exhibited good electrical conductivity after depositing on micro-electrode templates. Moreover, nanowires exhibit some sensing properties for CO. However, because of the slow saturation of CO adsorption, the response speed of the sensor is slow. In order to solve this problem, Zhang et al. [34] also prepared PEDOT: PSS/PVP nanofibers (1.8 g of PVP dissolved into 8.2 g of ethanol with the addition of 1.1 g of PEDOT:PSS). Further, the use of the ultra-sensitive quartz crystal microbalance (QCM) for CO sensing improved the sensing performance, as shown in Figure 4(a) and (b). In contrast, ammonia gas

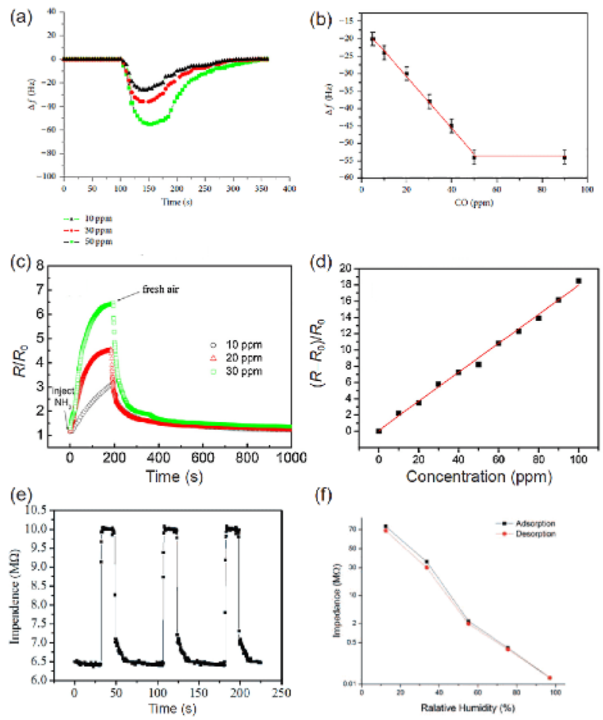

Figure 4 (Color online) (a) Response curve of PEDOT:PSS/PVP nanofibers to CO and (b) their sensitivity to different concentrations [34]; (c) resistivity change of polyaniline/PMMA composite nanofibers at different ammonia concentrations and (d) their sensitivity [35]; (e) humidity response curve of $BaTiO_3$ nanowires and (f) their recovery performance curve. The humidity response curve is a resistance change diagram in 33% and 97% humidity environments [36].

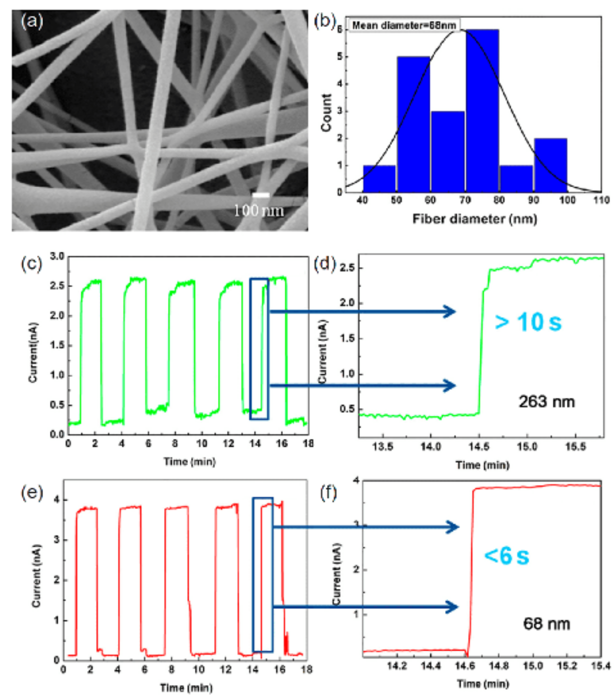

Figure 5 (Color online) (a) Scanning electron microscopy (SEM) image of nanofibers obtained by using ultrahigh voltage electrospinning; (b) the diameter profile of the nanofibers, with an average diameter of 68 nm, while the conventional electrospinning obtained fibers with a diameter of 263 nm; (c), (d) ammonia sensing response plots for conventional fibers with a response time greater than 10 s; (e), (f) ammonia sensing response plot of nanofibers with a response time of less than 6 s [37].

causes a change in the electrical resistance of polyaniline. Meanwhile, Zhang et al. [35] prepared poly(methyl methacrylate) (PMMA) fibers by electrospinning (PMMA dissolved into tetrahydrofuran with a weight ratio of 20%) and then polymerized polyaniline on the surface to fabricate conductive fibers. These fibers exhibited the good sensing properties of ammonia gas, as shown in Figure 4(c) and (d) [35]. Sheng et al. [36] obtained inorganic nanofibers of barium titanate by calcining the precursor. This fiber exhibited moisture sensing properties, as shown in Figure 4(e) and (f).

In contrast, reducing the size of the fiber further improved the sensing performance. With the low-current measurement technology, unpercolated, high-resistance fibers can also exhibit good gas sensing performance, which may be attributed to the gas response in non-conductive areas. Zhang et al. [37] prepared finer fibers than those obtained by conventional electrospinning by connecting a negative high-voltage source to the collecting electrode. The average size of these PEDOT:PSS/PVA fibers reached 68 nm, and most of the fiber diameters were below 100 nm, as shown in Figure 5(a) and (b). Comparative experiments showed that the reduction in fiber diameter could effectively improve the response speed. In terms of the saturation response time, the response time of the 68-nm fiber was less than 6 s, while the response time of the conventional electrospun fiber was more than 10 s, as shown in Figure 5(c)–(f) [37].

Note that Zhang et al. [28] found that a silver-loaded sodium alginate fiber prepared by the reduction method contains the conductive material uniformly distributed inside and outside the fiber, and the conductive fiber has good humidity response characteristics. Figure 6(b) shows that the current signal is smooth during normal breathing. As the breathing increases during running, the current signal gradually increases, indicating that more gas is being exhaled. As the gas exhaled by the human body contains a large amount of water vapor, the resistance of the sensor becomes small, resulting in an increase in the current under an electric constant voltage state. Our experimental results showed that this humidity sensor had a high signal-to-noise ratio, so it has also been used in the attempts to characterize the emotional state of the wearer. Figure 6(c) and (d) shows that the current increases slightly under different emotional conditions. In the case of delight, the wearer's laugh causes different shades of breathing, which are manifested in the current, that is, the complexity of the wave pattern. In the case of sorrow, the wearer's continuous and steady sobs make the output signal a stable waveform. In daily life, deaths due to acute respiratory arrest are a threat to human life, and if these signals are alerted, it is easy to save the lives of these respiratory ar-

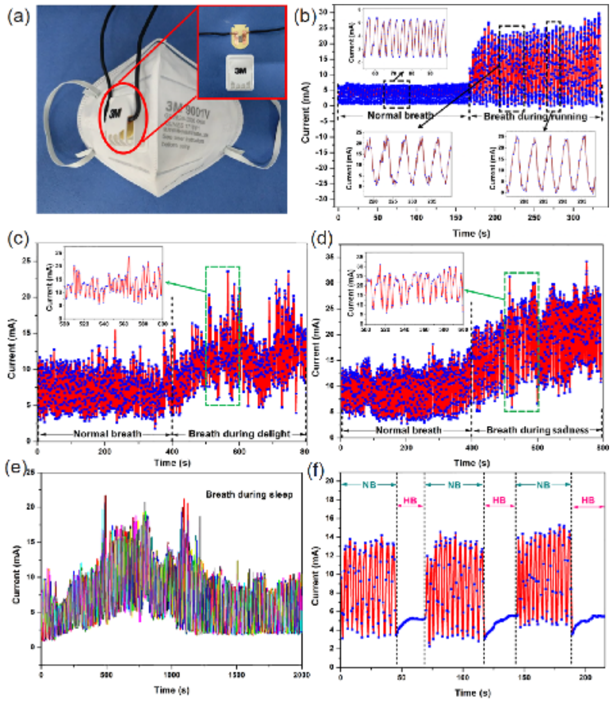

Figure 6 (Color online) (a) Image of the mask-integrated silver-loaded sodium alginate fiber; (b) response signal diagrams for different breathing depth conditions; (c), (d) comparison of response signals under different emotions; (e) corresponding signal conditions during normal sleep; (f) comparison of signals in the case of hard breathing (HB) and normal breathing (NB) [28].

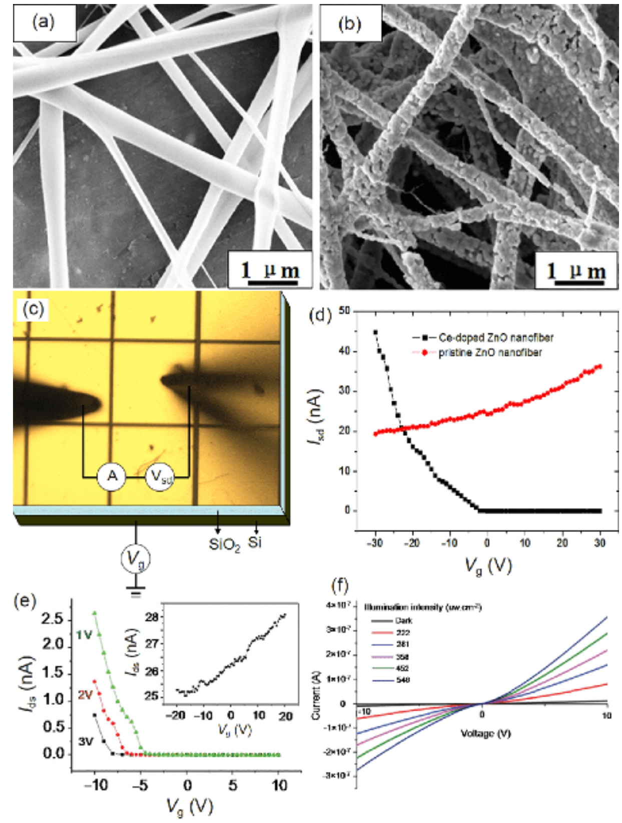

Figure 7 (Color online) (a), (b) SEM image comparison of doped ZnO fibers before and after sintering [40]; (c) field effect test configuration of ZnO fiber [40]; (d) transfer characteristics of Ce-doped ZnO [40]; (e) transfer characteristics of La-doped ZnO [38]; (f) *I-V* curve of La-doped ZnO under different wavelengths of light [38].

resters. Figure 6(e) and (f) shows this application. In the right situation, the wearer exhibits normal breathing (NB), as shown in Figure 6(e). However, in the case of hard breathing (HB), the output signal is significantly smoothed and reduced. A timely warning can be provided by using a simple threshold delay algorithm or a machine learning algorithm [28].

3.3 Photodetector

Semiconductor materials, particularly narrow-bandgap semiconductor materials, tend to respond well to light. Visible light with sufficient energy can excite carriers to the conduction band, increasing the carrier concentration, eventually leading to an increase in conductivity, as evidenced by a significant decrease in resistance with illumination, which can characterize the light intensity. Zhang et al. [38] used a zinc oxide precursor containing a polymer material (1.5 g of PVP, 1.0 g of zinc acetate, and 0.2 g of lanthanum acetate were mixed with 8.5 g of ethanol and 0.2 g of deionized water) to obtain a zinc oxide inorganic nanofiber. After doping rare earth elements such as La and Ce in the ZnO nanofibers [38,39], the researchers found that doping changed the intrinsic n-type ZnO semiconductors to p-type semiconductors. These semiconductors responded well to light, as shown in Figure 7 [38,40]. Liu et al. [41] used a near-field electrospinning device to print arrays of ZnO nanowires that exhibited ultra-high detection performance, as shown in Figure 8.

3.4 Conductive wire

Note that the nanofibers can form a good conductive wire. Tong et al. [42] fabricated a conductive wire by coating carbon nanotubes onto a yarn obtained by twisting an electrospun membrane, as shown in Figure 9 [42]. The twisting process was invented by Zheng et al [43]. It works well as an ordinary conductive wire and can be hidden into black clothes, which can be a good support to the future smart fabric [42].

3.5 Smart nanogenerator

In the recent years, nanogenerators have attracted increasing attention. As nanosystems are less compatible with traditional power supply technologies, the use of self-powered systems based on nanogenerators is a good choice. Nanogenerators are sufficiently small to convert mechanical energy into electrical energy and are therefore particularly

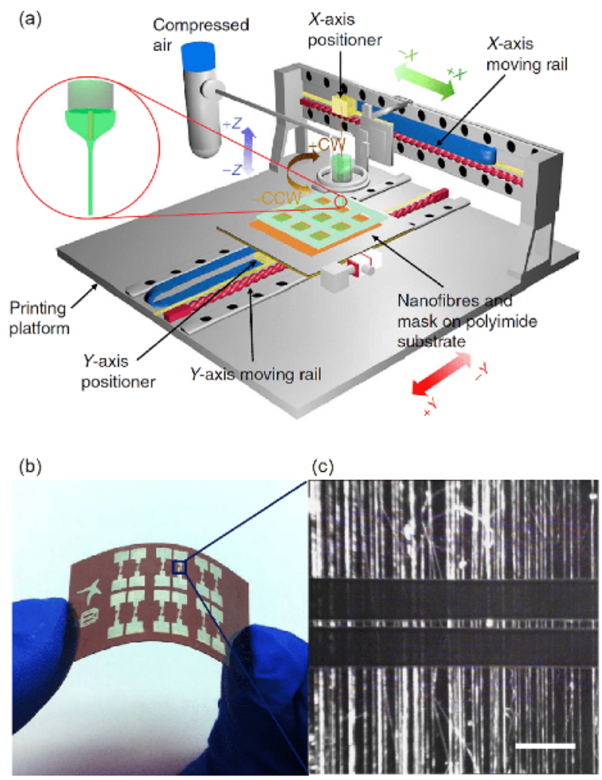

Figure 8 (Color online) Near-field printing of zinc oxide nanowire photosensor arrays. (a) Schematic representation of the device for nanowire printing; (b) flexibility demonstration of the nanowire arrays; (c) optical photograph of a nanowire array with a scale bar of 30 μm [41].

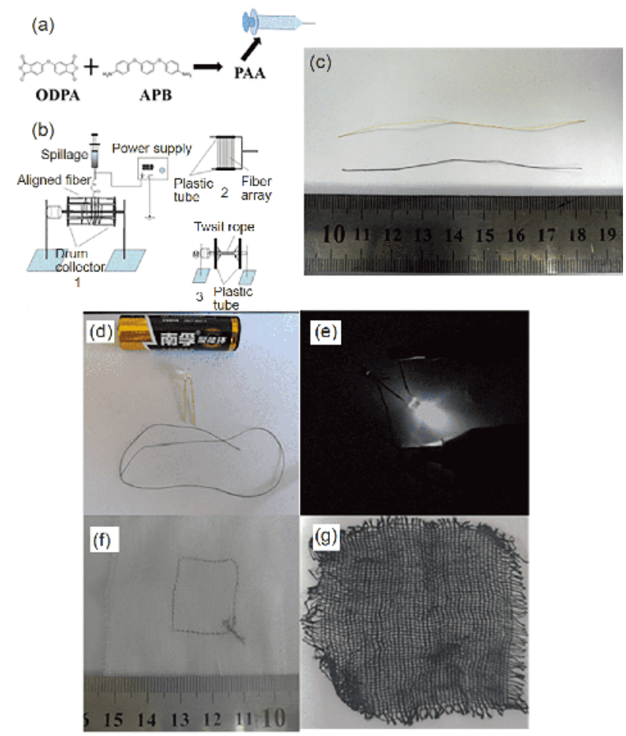

Figure 9 (Color online) Invisible wire prepared by electrospinning. (a), (b) Preparation of the nano-strand; (c) schematic representation of the original stranded wire and the wire deposited by carbon nanotubes; (d), (e) use of a conductive wire to power the LED; (f), (g) effect of weaving the wire on white and black cloth; the nanowire is unnoticeable on the black cloth [42].

suitable for wearable devices. In contrast, its output intensity tends to change significantly with pressure, temperature, and so on, so it can be used as an excellent self-powered sensor. Guo et al. [44] integrated the Bluetooth wireless transceiver module to connect this self-powered sensor to a mobile phone, realizing a connection between the smart fabric and an intelligent terminal. Piezoelectric nanogenerators can produce an electrical output under pressure, as shown in Figure 10. The higher the pressure is, the stronger is the output, which can be used for self-powered pressure sensing. In contrast, the piezoelectric polymer material has a pyroelectric output property; thus, a corresponding response electrical signal is generated when the temperature changes. It is very important that the current output signals of the two do not interfere with each other but output simultaneously in a signal superimposed manner, which results in the simultaneous transduction of the pressure signal and the temperature signal, as shown in Figure 11. Note that the most important sensing properties of human skin are pressure sensing and temperature sensing. Wang et al. [45] further reduced the configuration of the piezoelectric self-powered sensing system to obtain a bionic single-electrode electronic skin unit. This single-electrode electronic skin unit not only retains the basic sensing capabilities of the piezoelectric self-powered sensor but can also be made in a flexible form or in a transparent form, as shown in Figure 12. Further research has shown that this single-electrode electronic skin has a stronger resistance to a short circuit than the conventional electronic skin, as shown in Figure 13 [45].

4 Summary and outlook

With the development of technology, electronic products will gradually shift from smart terminals to micro-wearable devices, and smart fabrics with sensing performance will become an important development prospect. In this regard, the electrospinning technology has an irreplaceable advantage in the preparation of continuous nanowires. On one hand, environmentally friendly materials can be introduced [46,47]. On the other hand, because of the simplicity of the technology, electrospinning can be well modified to prepare nanostructures with different morphologies, thereby expanding different functions. Combined with other conductor preparation methods, such as electrochemical deposition [48,49] and flash light irradiation, more designs can be achieved [50]. Considering the difficulty of compatibility between the nanotechnology and the traditional power supply system, the self-powered nanogenerator sensing system will become a good choice for smart fabrics. However, a

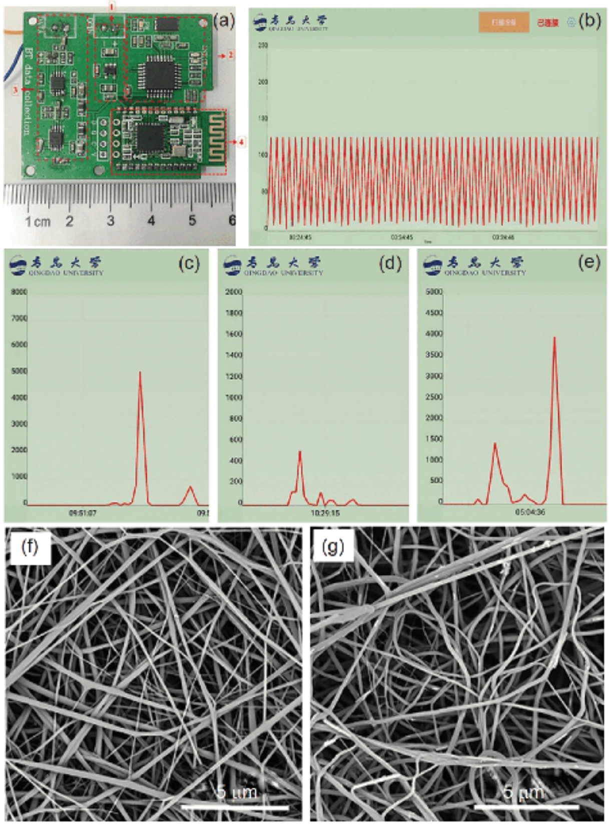

Figure 10 (Color online) (a) Schematic representation of the bluetooth system used for wireless transmission; (b) static perturbation signal; (c)–(e) wireless signals when picking up, walking, and running; (f) SEM image of pure PVDF fibers; (g) SEM image of PVDF doped by $BaTiO_3$ nanowires [44].

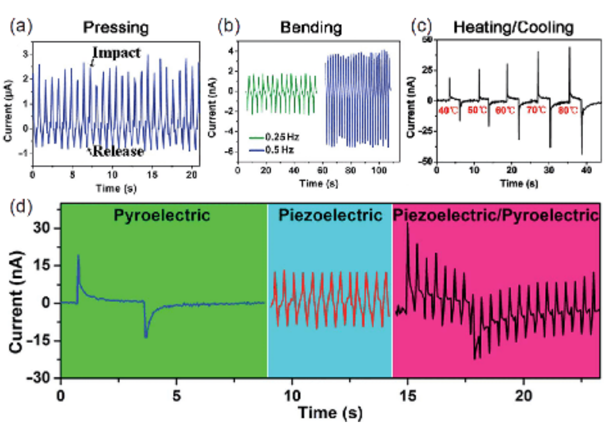

Figure 11 (Color online) PVDF fiber membrane performance. (a) Piezoelectric response current under pressure; (b) piezoelectric response current under bending; (c) pyroelectric current due to temperature changes; (d) simultaneous use of pressure and temperature superimpose the two current signals [6].

truly practical self-powered nanosystem must solve the problem of self-powered wireless signal output in order to establish an interface with future IoT systems. Meanwhile, a biocompatible nanofabric can be joined with an artificial scaffold material to sense vital signs such as blood pressure, body temperature, and blood sugar concentration variation in the human body, and provide more detailed physiological indicators for the human body through continuous data collection.

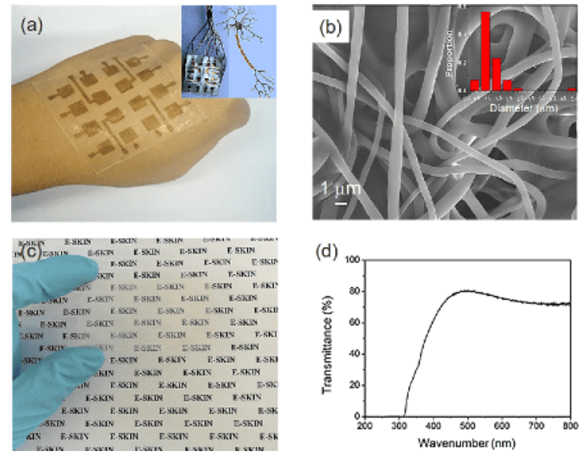

Figure 12 (Color online) PVDF single-electrode electronic skin display. (a) Skin attachment; the insert is the wiring diagram at work and its comparison with neurons; (b) SEM image and diameter distribution of the nanofibers; (c) transparency demonstration of the electronic skin deposited on the indium stannate (ITO) surface and (d) its transmission spectrum [45].

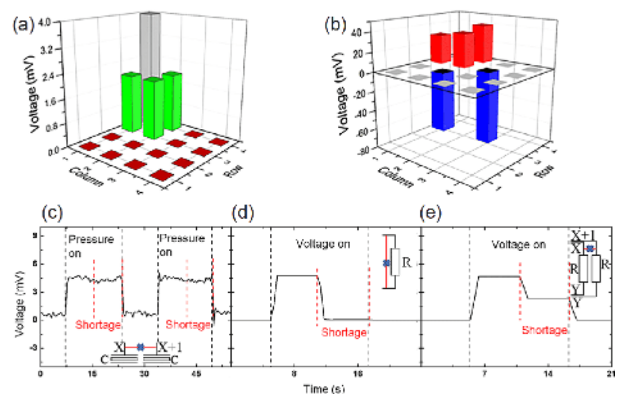

Figure 13 (Color online) (a) Pressure map and (b) hot and cold map of the single-electrode electronic skin; (c) short circuiting of adjacent elements of a single-electrode electronic skin element has no effect on the output signal. For the resistance sensing unit. (d) Short circuit of the component itself and (e) the short circuit of the neighboring component causes an error signal output [45].

Microstructure improvement is an indispensable task in the preparation of nanosensors using the electrospinning technology. Through the improvement of the electrospinning technology itself, the fiber diameter can be continuously reduced [51–53], thereby leading to a higher specific surface area; therefore, sensors with better performance can be obtained by utilizing these techniques. Alternatively, the preparation of the hollow structure in combination with the Kirkendall effect can further increase the specific surface area of the fiber [54–56]. Of course, a more variable choice is to prepare a two-dimensional material-bonded hierarchical structure through reasonable surface modification.

Currently, fiber deposition should be better controlled so as to achieve the production of inexpensive and large-scale sensors in the future, and the solution to this problem is not difficult. Electrospinning can easily and controllably prepare one-dimensional nanowires. Whether it is a near-field electrospinning technique combined with a motion console [57,58] or an ordered fiber collection technique using a high-speed rotating collector [59–61], parallel nanofiber arrays or cross-nanofiber arrays can be well prepared. Using these techniques, inexpensive mapping functions can be realized, thereby realizing certain imaging technologies such as inexpensive touch plates, image sensors, and even gas concentration distribution sensors, providing a certain medical imaging technology reserve. In contrast, multi-channel signal acquisition can achieve its own repeatability verification and regression analysis through a functional circuit, so as to better ensure the accuracy of the sensing signal. In addition, because of the flexibility of supporting the nanostructure, electrospun nanofiber-based flexible electronic devices tend to have higher flexibility and thinner thickness, which will also result in a good performance in the field of flexible electronic devices.

This work was supported by the National Natural Science Foundation of China (Grant No. 51673103), and the Facility Horticulture Laboratory of Universities in Shandong Program (Grant No. 2018YY053). We thank LetPub (www.letpub.com) for its linguistic assistance during the preparation of this manuscript.

1 Cordero-Edwards K, Domingo N, Abdollahi A, et al. Ferroelectrics as smart mechanical materials. Adv Mater, 2017, 29: 1702210
2 Kim S H, Das M P. Understanding metamaterials in the realm of smart materials. Adv Mater, 2018, 2005: 020011
3 Bai W, Jiang Z, Ribbe A E, et al. Smart organic two-dimensional materials based on a rational combination of non-covalent interactions. Angew Chem Int Ed, 2016, 55: 10707–10711
4 Yu X, Cheng H, Zhang M, et al. Graphene-based smart materials. Nat Rev Mater, 2017, 2: 17046
5 Shen H, Li L, Xu D. Preparation of one-dimensional SnO_2-In_2O_3 nano-heterostructures and their gas-sensing property. RSC Adv, 2017, 7: 33098–33105
6 You M H, Wang X X, Yan X, et al. A self-powered flexible hybrid piezoelectric-pyroelectric nanogenerator based on non-woven nanofiber membranes. J Mater Chem A, 2018, 6: 3500–3509
7 Pyo J Y, Cho W J. In-plane-gate a-IGZO thin-film transistor for high-sensitivity pH sensor applications. Sens Actuat B-Chem, 2018, 276: 101–106
8 You M H, Yan X, Zhang J, et al. Colorimetric humidity sensors based on electrospun polyamide/$CoCl_2$ nanofibrous membranes. Nanoscale Res Lett, 2017, 12: 360
9 Sui J X, Wang X X, Song C, et al. Preparation and low-temperature electrical and magnetic properties of $La_{0.33}Pr_{0.34}Ca_{0.33}MnO_3$ nanofibers via electrospinning. J Magn Magn Mater, 2018, 467: 74–81
10 Zhang J, Li S, Ju D D, et al. Flexible inorganic core-shell nanofibers endowed with tunable multicolor upconversion fluorescence for simultaneous monitoring dual drug delivery. Chem Eng J, 2018, 349: 554–561
11 Li S, Zhang J, Ju D D, et al. Flexible inorganic composite nanofibers with carboxyl modification for controllable drug delivery and enhanced optical monitoring functionality. Chem Eng J, 2018, 350: 645–652
12 Chen S, Long Y Z, Zhang H D, et al. Fabrication of ultrathin In_2O_3 hollow fibers for UV light sensing. Phys Scr, 2014, 89: 115808
13 Chen S, Yu M, Han W P, et al. Electrospun anatase TiO_2 nanorods for flexible optoelectronic devices. RSC Adv, 2014, 4: 46152–46156
14 Zhang Z, Schwanz D, Narayanan B, et al. Perovskite nickelates as electric-field sensors in salt water. Nature, 2018, 553: 68–72
15 Wang X, Zhang Y, Zhang X, et al. A highly stretchable transparent self-powered triboelectric tactile sensor with metallized nanofibers for wearable electronics. Adv Mater, 2018, 30: 1706738
16 Han S T, Peng H, Sun Q, et al. An overview of the development of flexible sensors. Adv Mater, 2017, 29: 1700375
17 Fennimore A M, Yuzvinsky T D, Han W Q, et al. Rotational actuators based on carbon nanotubes. Nature, 2003, 424: 408–410
18 Haines C S, Lima M D, Li N, et al. Artificial muscles from fishing line and sewing thread. Science, 2014, 343: 868–872
19 Long Y Z, Li M M, Gu C, et al. Recent advances in synthesis, physical properties and applications of conducting polymer nanotubes and nanofibers. Prog Polymer Sci, 2011, 36: 1415–1442
20 Zhang Z G, Wang X X, Zhang J, et al. Recent advances in 1D micro- and nanoscale indium oxide structures. J Alloys Compd, 2018, 752: 359–375
21 Long Y Z, Duvail J L, Chen Z J, et al. Electrical properties of isolated poly(3,4-ethylenedioxythiophene) nanowires prepared by template synthesis. Polym Adv Technol, 2009, 20: 541–544
22 Yang H, Long Y Z,Ding H J Template-free synthesis and properties of polyaniline nanostructures doped with different oxidants. Nano-Scale Amourphous Mater, 2011, 688: 334
23 Long Y, Chen Z, Ma Y, et al. Electrical conductivity of hollow polyaniline microspheres synthesized by a self-assembly method. Appl Phys Lett, 2004, 84: 2205–2207
24 Liu L Z, Tian S B, Long Y Z, et al. Tunable periodic graphene antidot lattices fabricated by e-beam lithography and oxygen ion etching. Vacuum, 2014, 105: 21–25
25 Long Y, Zhang L, Ma Y, et al. Electrical conductivity of an individual polyaniline nanotube synthesized by a self-assembly method. Macromol Rapid Commun, 2003, 24: 938–942
26 He X X, Zheng J, Yu G F, et al. Near-field electrospinning: Progress and applications. J Phys Chem C, 2017, 121: 8663–8678
27 Si W Y, Zhang H D, Liu Y J, et al. Fabrication and pressure sensing analysis of ZnO/PVDF composite microfiber arrays by low-voltage near-field electrospinning. Chem J Chin Univ, 2017, 38: 997–1001
28 Zhang J, Wang X X, Zhang B, et al. *In situ* assembly of well-dispersed Ag nanoparticles throughout electrospun alginate nanofibers for monitoring human breath—smart fabrics. ACS Appl Mater Interfaces, 2018, 10: 19863–19870
29 Liu H, Zhang Z G, Wang X X, et al. Highly flexible Fe_2O_3/TiO_2 composite nanofibers for photocatalysis and utraviolet detection. J Phys Chem Solids, 2018, 121: 236–246
30 Zhang H D, Liu Y J, Zhang J, et al. Electrospun ZnO/SiO_2 hybrid nanofibers for flexible pressure sensor. J Phys D-Appl Phys, 2018, 51: 085102
31 Hu W P, Zhang B, Zhang J, et al. Ag/alginate nanofiber membrane for flexible electronic skin. Nanotechnology, 2017, 28: 445502
32 Yu G F, Yan X, Yu M, et al. Patterned, highly stretchable and conductive nanofibrous PANI/PVDF strain sensors based on electrospinning and *in situ* polymerization. Nanoscale, 2016, 8: 2944–2950
33 Zhang H D, Long Y Z, Li Z J, et al. Fabrication of comb-like ZnO nanostructures for room-temperature CO gas sensing application. Vacuum, 2014, 101: 113–117
34 Zhang H D, Yan X, Zhang Z H, et al. Electrospun PEDOT:PSS/PVP nanofibers for CO gas sensing with quartz crystal microbalance technique. Int J Polymer Sci, 2016, 2016: 1–6
35 Zhang H D, Tang C C, Long Y Z, et al. High-sensitivity gas sensors based on arranged polyaniline/PMMA composite fibers. Sens Actuat A-Phys, 2014, 219: 123–127
36 Sheng C H, Zhang H D, Chen S, et al. Fabrication, structural and

humidity sensing properties of $BaTiO_3$ nanofibers via electrospinning. Int J Mod Phys B, 2015, 29: 1550066
37 Zhang Q, Wang X, Fu J, et al. Electrospinning of ultrafine conducting polymer composite nanofibers with diameter less than 70 nm as high sensitive gas sensor. Materials, 2018, 11: 1744
38 Zhang H D, Yu M, Zhang J C, et al. Fabrication and photoelectric properties of La-doped p-type ZnO nanofibers and crossed p-n homojunctions by electrospinning. Nanoscale, 2015, 7: 10513–10518
39 Liu Y J, Zhang H D, Zhang J, et al. Effects of Ce doping and humidity on UV sensing properties of electrospun ZnO nanofibers. J Appl Phys, 2017, 122: 105102
40 Liu S, Liu S L, Long Y Z, et al. Fabrication of p-type ZnO nanofibers by electrospinning for field-effect and rectifying devices. Appl Phys Lett, 2014, 104: 042105
41 Liu X, Gu L, Zhang Q, et al. All-printable band-edge modulated ZnO nanowire photodetectors with ultra-high detectivity. Nat Commun, 2014, 5: 4007
42 Tong L, Wang X X, Zhu J W, et al. Conductive twisted polyimide composite nanofiber ropes with improved tensile strength, thermal stability and high flexibility. J Phys D-Appl Phys, 2018, 51: 485102
43 Zheng J, Yan X, Li M M, et al. Electrospun aligned fibrous arrays and twisted ropes: Fabrication, mechanical and electrical properties, and application in strain sensors. Nanoscale Res Lett, 2015, 10: 475
44 Guo W, Tan C, Shi K, et al. Wireless piezoelectric devices based on electrospun PVDF/$BaTiO_3$ NW nanocomposite fibers for human motion monitoring. Nanoscale, 2018, 10: 17751–17760
45 Wang X, Song W Z, You M H, et al. Bionic single-electrode electronic skin unit based on piezoelectric nanogenerator. ACS Nano, 2018, 12: 8588–8596
46 Hao L, Wang R, Zhao Y, et al. The enzymatic actions of cellulase on periodate oxidized cotton fabrics. Cellulose, 2018, 25: 6759–6769
47 Wang R, Yang C, Fang K, et al. Removing the residual cellulase by graphene oxide to recycle the bio-polishing effluent for dyeing cotton fabrics. J Environ Manage, 2018, 207: 423–431
48 Kai W. Electrodeposition synthesis of PANI/MnO_2/graphene composite materials and its electrochemical performance. Int J Electrochem Sci, 2017, 8306–8314
49 Wang K, Zhou S Z, Zhou Y T, et al. Synthesis of porous carbon by activation method and its electrochemical performance. Int J Electrochem Sci, 2018, 13: 10766–10773
50 Wang K, Pang J, Li L, et al. Synthesis of hydrophobic carbon nanotubes/reduced graphene oxide composite films by flash light irradiation. Front Chem Sci Eng, 2018, 12: 376–382
51 Huang C, Chen S, Lai C, et al. Electrospun polymer nanofibres with small diameters. Nanotechnology, 2006, 17: 1558–1563
52 Yang R, He J, Xu L, et al. Bubble-electrospinning for fabricating nanofibers. Polymer, 2009, 50: 5846–5850
53 Jian S, Zhu J, Jiang S, et al. Nanofibers with diameter below one nanometer from electrospinning. RSC Adv, 2018, 8: 4794–4802
54 Fu J, Zhang J, Peng Y, et al. Wire-in-tube structure fabricated by single capillary electrospinning via nanoscale Kirkendall effect: The case of nickel-zinc ferrite. Nanoscale, 2013, 5: 12551–12557
55 Ji W, Wei H, Cui Y, et al. Facile synthesis of porous forsterite nanofibres by direct electrospinning method based on the Kirkendall effect. Mater Lett, 2018, 211: 319–322
56 Zhang Z, Yang G, Wei J, et al. Morphology and magnetic properties of $CoFe_2O_4$ nanocables fabricated by electrospinning based on the Kirkendall effect. J Cryst Growth, 2016, 445: 42–46
57 Zheng J, Sun B, Long Y Z, et al. Fabrication of nanofibers by low-voltage near-field electrospinning. Adv Mater Res, 2012, 486: 60–64
58 Zheng J, Long Y Z, Sun B, et al. Polymer nanofibers prepared by low-voltage near-field electrospinning. Chin Phys B, 2012, 21: 048102
59 Doergens A, Roether J A, Dippold D, et al. Identifying key processing parameters for the electrospinning of aligned polymer nanofibers. Mater Lett, 2015, 140: 99–102
60 García-López E, Olvera-Trejo D, Velásquez-García L F. 3D printed multiplexed electrospinning sources for large-scale production of aligned nanofiber mats with small diameter spread. Nanotechnology, 2017, 28: 425302
61 Afifi A M, Yamamoto M, Yamane H, et al. Electrospinning and characterization of aligned nanofibers from chitosan/polyvinyl alcohol mixtures: Comparison of several target devices newly designed. FIBER, 2011, 67: 103–108